

# A cosmological exclusion plot: Towards model-independent constraints on modified gravity from current and future growth rate data

Laura Taddei<sup>1,2</sup>, Luca Amendola<sup>2</sup>

<sup>1</sup>*Dipartimento di Fisica e Scienze della Terra, Università di Parma, Viale Usberti 7/A, I-43100 Parma, Italy.* and  
<sup>2</sup>*Institut für Theoretische Physik, Ruprecht-Karls-Universität Heidelberg, Philosophenweg 16, 69120 Heidelberg, Germany.*

Most cosmological constraints on modified gravity are obtained assuming that the cosmic evolution was standard  $\Lambda$ CDM in the past and that the present matter density and power spectrum normalization are the same as in a  $\Lambda$ CDM model. Here we examine how the constraints change when these assumptions are lifted. We focus in particular on the parameter  $Y$  (also called  $G_{\text{eff}}$ ) that quantifies the deviation from the Poisson equation. This parameter can be estimated by comparing with the model-independent growth rate quantity  $f\sigma_8(z)$  obtained through redshift distortions. We reduce the model dependency in evaluating  $Y$  by marginalizing over  $\sigma_8$  and over the initial conditions, and by absorbing the degenerate parameter  $\Omega_{m,0}$  into  $Y$ . We use all currently available values of  $f\sigma_8(z)$ . We find that the combination  $\hat{Y} = Y\Omega_{m,0}$ , assumed constant in the observed redshift range, can be constrained only very weakly by current data,  $\hat{Y} = 0.28^{+0.35}_{-0.23}$  at 68% c.l. We also forecast the precision of a future estimation of  $\hat{Y}$  in a Euclid-like redshift survey. We find that the future constraints will reduce substantially the uncertainty,  $\hat{Y} = 0.30^{+0.08}_{-0.09}$ , at 68% c.l., but the relative error on  $\hat{Y}$  around the fiducial remains quite high, of the order of 30%. The main reason for these weak constraints is that  $\hat{Y}$  is strongly degenerate with the initial conditions, so that large or small values of  $\hat{Y}$  are compensated by choosing non-standard initial values of the derivative of the matter density contrast.

Finally, we produce a forecast of a cosmological exclusion plot on the Yukawa strength and range parameters, which complements similar plots on laboratory scales but explores scales and epochs reachable only with large-scale galaxy surveys. We find that future data can constrain the Yukawa strength to within 3% of the Newtonian one if the range is around a few Megaparsecs. In the particular case of  $f(R)$  models, we find that the Yukawa range will be constrained to be larger than 80 Mpc/h or smaller than 2 Mpc/h (95% c.l.), regardless of the specific  $f(R)$  model.

## I. INTRODUCTION

Testing possible modifications of gravity at very large scales is currently one of the most interesting research activity in cosmology. Modifications of standard gravity are often modeled by introducing one or more additional mediating fields in the gravitational Lagrangian. One of the most well studied example is the so-called Horndeski theory, which adds to the Einstein-Hilbert Lagrangian a single scalar field that obey the most general second order equation of motion [1].

As shown in several papers (e.g. [2–5]), a generic modification of gravity introduces at linear perturbation level two new functions that depend only on background time-dependent quantities and, in Fourier space, on the wavenumber  $k$ . One function, that we denote here with  $Y(t, k)$  (sometimes also called  $G_{\text{eff}}$ ), modifies the standard Poisson equation, while the second one,  $\eta(t, k)$ , the anisotropic stress or tilt, provides the relation between the two gravity potentials  $\Psi, \Phi$ . In standard gravity, one has  $Y = \eta = 1$ .

In the so-called quasi-static regime (i.e. for linear scales that are below the sound horizon) of the Horndeski models, and also in some cases [6] of bimetric models [7], the two functions  $Y, \eta$  take a particularly simple form and can be directly constrained through observations [8, 9]. In particular, one can use observations of weak lensing, redshift distortions and galaxy clustering to constrain or detect modifications of gravity at cosmological scales [10].

One problem of these techniques is that often one makes explicitly or implicitly several assumptions that might not be warranted by current data. For instance, one often assumes that the behavior of the cosmological model before dark energy domination, i.e. essentially at any time except very recently, is the standard radiation and matter dominated universe. While we have at least some proof that the radiation epoch had to be close to standard, otherwise one would see deviations from the standard big bang nucleosynthesis and on the microwave background sky, we have much less robust data concerning the matter dominated era, in particular between decoupling and now. For instance, models in which the dark energy was a substantial fraction of the cosmic energy at high redshift [11, 12] cannot yet be excluded.

We identify in particular three assumptions that are very commonly made (at least one of them is included in, for instance, [13–20]) and which are certainly acceptable in some cases but that, in reality, are not necessarily warranted in more general gravity theories. First, we do not know what is the present value of the matter density fraction  $\Omega_{m,0}$ . If we take it from distance measurements (supernovae, baryon acoustic oscillation) then one should be aware

that the observed quantity is the expansion rate  $H(z)$  and not the equation of state  $w(z)$  or  $\Omega_{m,0}$ . In fact, the EOS  $w(z)$  depends on assuming a value of  $\Omega_{m,0}$ , and viceversa [21]. Of course if  $w(z)$  is parametrized by a small number of parameters then one can get also  $\Omega_{m,0}$  from the distance data, but the estimation will depend on the chosen parametrization. Moreover,  $\Omega_{m,0}$  cannot be determined without ambiguity with other techniques, e.g. from weak lensing (e.g. [22]) or  $X$ -ray temperature in clusters (e.g. [23]), since these estimates always assume standard Newtonian gravity.

Second, we do not know what is the present value of the power spectrum amplitude  $\sigma_8$ . In fact, any estimate of  $\sigma_8$ , through e.g. weak lensing (see e.g. [22]), cosmic microwave background (e.g. [24]), or cluster abundances (see e.g. [23], [25]), depends again on assuming a particular (normally, Newtonian), theory of gravity.

Third, when we obtain the theoretical behavior of the linear perturbation, by integrating the matter conservation equations, we need to assume some initial condition for the matter density contrast  $\delta_m$  and the peculiar velocity divergence  $\theta_m$  (or equivalently on  $\delta_m$  and  $\delta'_m$ , the prime being from now on the derivative with respect to the e-folding time  $N = \log a$ ). Typically, this problem is bypassed assuming that the evolution in the past (say, for redshifts  $z \gg 1$ ) was identical to a matter dominated universe so that  $\delta_m \sim a$  and  $\delta'_{in} = \delta_{in}$  (of course since we are in the linear regime one can always choose freely one of the two initial conditions, say  $\delta_{in}$ ). However, if we do not know the cosmological model in the past, we cannot fix  $\delta'_{in}$ . For instance, in some coupled dark matter-dark energy model the perturbations grow faster than in  $\Lambda$ CDM during the matter epoch due to the fact that the dark energy field is not negligible (e.g. [26]); in this case  $\delta'_{in} > \delta_{in}$ . Similarly, in a Brans-Dicke model with coupling  $\omega$  one has  $\delta'_{in} = (2+\omega)\delta_{in}/(1+\omega)$  [27]; although  $\omega$  has to be very large to pass local gravity constraints, if a screening mechanism is present these bounds becomes very weak.

In this paper we wish to examine what constraints one can still get on modified gravity, in particular on  $Y$ , when all three assumptions, on  $\Omega_{m,0}$ ,  $\sigma_8$  and  $\delta'_{in}$ , are lifted by marginalizing over all the non-degenerate parameters. We will consider both current data and forecasted data from a future experiment that approximates the Euclid[28] survey [29]. We call this a model-independent approach, although of course we are still making several model-dependent assumptions, like for instance that we are really dealing with linear scales in the sub-horizon regime and that matter is conserved. We also assume for simplicity that matter is a pressureless fluid and that the background is well approximated by a  $\Lambda$ CDM behavior during the redshift range that we consider, although both these assumptions can be easily generalized. One has also to bear in mind that it is possible to modify gravity leaving the function  $Y$  unaltered (but not  $\eta$ , when properly defined in the Jordan frame, see discussion in [30]) so that even finding  $Y = 1$  does not guarantee Einsteinian gravity.

We use the  $f\sigma_8(z)$  data obtained through the redshift distortion method [31] and collected in [17, 22]. This method does not rely on assuming standard gravity, contrary to methods based, for instance, on extrapolation from CMB data, on weak lensing, cluster abundances, or galaxy power spectra.

The conclusion is that both present and future data have little chance to set stringent constraints on  $Y$  if one wants to be as much model-independent as possible. We find in particular a strong degeneracy between the initial conditions and  $Y$  that allows both relatively large and small values of  $Y$ . It is important to remark that we simplified our task by setting  $Y$  constant in time (the space dependence is either ignored as well or introduced according to the Horndeski model, see below). If we include an arbitrary time dependence, then the constraints would evaporate completely for current data, since we would have one datum at each redshift and one free parameter per redshift *plus* initial conditions and  $\sigma_8$ . For future data, where one can in principle obtain several data points at different  $k$ 's for each redshift, the constraints would not disappear but weaken a lot, and even more so if the initial conditions are taken to be  $k$ -dependent. Clearly, obtaining any constraint at all would be totally impossible if the  $Y$  function, instead of being restricted to follow the Horndeski form, were a completely arbitrary function of time and space.

This leaves one only two escape routes to obtain stronger constraints on modified gravity through cosmological observations at linear scales. The first one is to forget model-independency and assume specific modified gravity models. Then one can estimate the model-specific  $\sigma_8$ ,  $\Omega_{m,0}$  and the initial conditions and confine  $Y$  within a much narrower region. The second one is to use a different parameter to test modified gravity. In Ref. [32] it has been shown that the anisotropic parameter  $\eta$  is a useful probe of gravity since it is independent of  $\sigma_8$  and it can be estimated from observations through an algebraic relation, i.e. without the need of choosing initial conditions. It is moreover more deeply connected to modifications of gravity (rather than just clustering of dark energy) than  $Y$  [30]. Due to these properties,  $\eta$  can be estimated by future clustering and lensing data (or even from B-modes of the cosmic microwave background data [33, 34]) to a precision of just one percent if assumed constant [10]. This is to be contrasted to the 30% relative errors that can be obtained on the combination  $\Omega_{m,0}Y$  when model-independency is at least partially taken into account.

## II. THE HORNDESKI PARAMETERS

We are interested in the evolution of linear perturbations in the quasi-static limit (i.e. for scales significantly inside the cosmological horizon,  $k/(aH) \gg 1$ , and inside the Jeans length of the scalar,  $c_s k/(aH) \gg 1$ , such that the terms containing  $k$  dominate over the time-derivative terms). One has then the following equation of linear perturbation growth

$$\delta_m'' + (2 + \frac{E'}{E})\delta_m' = \frac{3}{2}\Omega_m\delta_m Y(a, k) \quad (1)$$

where  $\Omega_m = \Omega_{m0}a^{-3}/E^2$  and  $E \equiv H/H_0$ . The prime denotes the derivative respect to  $N \equiv \ln(a)$ . The function  $Y$ , the effective gravitational constant for matter, is defined as

$$Y(a, k) = -\frac{2k^2\Psi}{3(aH)^2\Omega_m\delta_m} \quad (2)$$

In this paper we always assume either that baryons do not feel modified gravity or that the local gravity experiments occur in an environment where the extra force is not felt; in either case, they do not set any useful constraint on the cosmological expression for  $Y$ .

Now we assume that the background is described by the  $\Lambda$ CDM model, so we have:

$$E^2 = \Omega_{m,0}^{(bg)}a^{-3} + 1 - \Omega_{m,0}^{(bg)} \quad (3)$$

where we distinguish here between the parameter  $\Omega_{m,0}^{(bg)}$  that enters the background rate  $E$  and the parameter  $\Omega_{m,0}$  that expresses the amount of clustered matter in Eq. (1). In a modified gravity theory, the two quantities are independent and should be clearly distinguished. A perfect knowledge of the expansion rate, e.g. through supernovae Ia, will determine  $E$  and, if the particular form (3) is assumed,  $\Omega_{m,0}^{(bg)}$  but says nothing about the clustered fraction of matter  $\Omega_{m,0}$ . For instance, if dark energy mediates an extra force, matter will not dilute as  $a^{-3}$  and the value of  $\Omega_{m,0}^{(bg)}$  that one would obtain from (3) would be unrelated to the real matter content.

The Horndeski Lagrangian is the most general Lagrangian for a single scalar field which gives second-order equations of motion for both the scalar field and the metric on an arbitrary background. In the quasi-static limit of the Horndeski Lagrangian one obtains:

$$Y = h_1 \frac{1 + (k/k_p)^2 h_5}{1 + (k/k_p)^2 h_3} \quad (4)$$

where  $h_1, h_3, h_5$  are time dependent functions that can be explicitly obtained when the full Horndeski Lagrangian is given [9]. The scale  $k_p$  is an arbitrary pivot scale that we choose to be  $k_p = 1h/\text{Mpc}$ .

Eq. (1) can be written as

$$\delta_m'' + (2 + \frac{E'}{E})\delta_m' = \frac{3}{2} \frac{\delta_m}{a^3 E^2} \Omega_{m,0} Y \quad (5)$$

This shows immediately that  $\Omega_{m,0}$  is fully degenerate with  $Y$ . In the following therefore we will only be able to constrain the quantity

$$\hat{Y} \equiv \Omega_{m,0} Y \quad (6)$$

Since our reference model is  $\Lambda$ CDM with  $\Omega_{m,0}^{(bg)} = 0.3$ , the standard value of  $\hat{Y}$  is 0.3. Similarly, when we take the specific Horndeski form (4), we will constrain the combination  $\hat{h}_1 \equiv \Omega_{m,0} h_1$ .

Now, the rate  $E$  itself can be estimated with distance indicators only up to some uncertainty. In the following however we will simplify our task by assuming that the error on  $E$  is actually already now negligible with respect to the errors on the other observational data. For current data this is not completely true so our estimate of the uncertainty on  $Y$  is actually a lower limit. As the main effect of a change in  $E$  is through the left-hand-side factor  $E^{-2}$  in Eq. (5), one can estimate the additional error on  $\hat{Y}$  induced by an error  $\Delta E$  in  $E$  to be  $|\Delta \hat{Y}|/\hat{Y} \approx 2|\Delta E|/E$ , to be added in quadrature. Current supernovae can determine  $E$  around  $z \approx 1$  with a relative error of 5-10%, so we can estimate an additional error on  $\hat{Y}$  around 10-20%. Since the uncertainty we find is quite larger than this, we

neglect the additional source of error from  $E$ . For the future data, one can indeed assume that  $E$  will be pretty fairly well determined up to better than a percent accuracy with future surveys and our lower limit will be closer to reality.

For the initial conditions on  $\delta_m$ , we fix the irrelevant value  $\delta_{in} = e^{N_{in}}$  with  $N_{in} = -1.5$  i.e.  $z_{in} \approx 3.5$ , while for the initial growth rate parameter  $\alpha = \delta'_{in}/\delta_{in}$  we either fix it to unity (standard  $\Lambda$ CDM) or adopt a uniform prior large enough to cover all the region in which the likelihood is significantly different from zero.

Two caveats are in order. First, the entire analysis of this paper deals with linear scales. However, the data points we employ are obtained averaging over various scales that include probably also some weakly non-linear region of the power spectrum. For instance, the effective wavenumber in the analysis of Ref. [35] is given as  $k_{\text{eff}} = 0.178h/\text{Mpc}$ , which at the average redshift of 0.57 is marginally affected by non linearity. In Ref. [18] the analysis of the same data including only large linear scales leads to an estimate of  $f\sigma_8(z)$  which is consistent with, and only mildly more uncertain than, the one obtained including smaller scales, indicating that the non linear effects are still subdominant. In any case, properly dealing with non linearity would require a reanalysis of the raw clustering data and an estimate of the non-linear corrections to  $\delta_m$  for non-standard model. Secondly, the data points have been obtained by assuming a particular background expansion in order to convert from redshift to distances. Here we assume a fiducial  $\Lambda$ CDM background with  $\Omega_{m,0} = 0.3$  which does not coincide exactly with the one employed in some of the real data analysis. The corrections induced by both the non-linear effects and the fiducial background mismatch are expected to be quite smaller than the rather large error that we obtain on our modified gravity parameters.

### III. MARGINALIZATION OVER $\sigma_8$

We build a data posterior by using two datasets, the *current dataset* and the *forecast dataset*. The current dataset includes all the independent published estimates of  $f\sigma_8(z)$  obtained with the redshift distortion method. It includes the data from 2dFGS, 6dFGS, LRG, BOSS, CMASS, WiggleZ and VIPERS, and spans the redshift interval from  $z = 0.07$  to  $z = 0.8$ , see Table I (see also [17, 22]). In some case the correlation coefficient between two samples has been estimated in Ref. [17] and included in our analysis; when there are different published results from the same dataset in Table I we include only the more recent one. The forecast dataset approximates instead the accuracy of a future Euclid mission [29, 36] and it has been obtained in Ref. [10] in the range from  $z = 0.5$  to  $z = 2.1$ . The growth rate data are given as a set of values  $d_i$  at various redshifts, where

$$d_i = f(z_i)\sigma_8(z_i) = f(z_i)\sigma_8 G(z_i) = \sigma_8 \frac{\delta'}{\delta_0} \quad (7)$$

and where  $f(z) = \delta'_m/\delta_m$  is the growth rate,  $G(z)$  is the growth factor normalized to unity today and  $\sigma_8$  is the present power spectrum normalization. We denote our theoretical estimates as  $t_i = \delta'_i/\delta_0$ . We build then the  $\chi^2$  function

$$\bar{\chi}_{f\sigma_8}^2 = (d_i - \sigma_8 t_i) C_{ij}^{-1} (d_j - \sigma_8 t_j) \quad (8)$$

where  $C_{ij}$  is the covariant matrix of the data. The first step to implement our model-independent estimates is to marginalize over  $\sigma_8$ , since as already mentioned to estimate its value from current data one would need to know the gravitational theory. Marginalizing the likelihood  $L' = \exp(-\bar{\chi}_{f\sigma_8}^2/2)$  over  $\sigma_8 > 0$  with uniform prior leads to a new posterior  $L = \exp(-\bar{\chi}_{f\sigma_8}^2/2)$  where

$$\chi_{f\sigma_8}^2 = S_{dd} - \frac{S_{dt}^2}{S_{tt}} + \log S_{tt} - 2 \log(1 + \text{Erf}(\frac{S_{dt}}{\sqrt{2S_{tt}}})) \quad (9)$$

and where

$$S_{dt} = d_i C_{ij}^{-1} t_j \quad (10)$$

$$S_{dd} = d_i C_{ij}^{-1} d_j \quad (11)$$

$$S_{tt} = t_i C_{ij}^{-1} t_j \quad (12)$$

This is the posterior distribution we will use in the following discussion.

Survey	z	$f(z)\sigma_8(z)$	References
6dFGRS	0.067	$0.423 \pm 0.055$	Beutler et al. (2012) [37]
LRG-200	0.25	$0.3512 \pm 0.0583$	Samushia et al (2012) [38]
	0.37	$0.4602 \pm 0.0378$	
LRG-60	0.25*	$0.3665 \pm 0.0601$	Samushia et al (2012) [38]
	0.37*	$0.4031 \pm 0.0586$	
BOSS	1) 0.30	$0.408 \pm 0.0552, \rho_{12} = -0.19$	Tojeiro et al. (2012) [39]
	2) 0.60	$0.433 \pm 0.0662$	
WiggleZ	1) 0.44	$0.413 \pm 0.080, \rho_{12} = 0.51$	Blake (2011) [40]
	2) 0.60	$0.390 \pm 0.063, \rho_{23} = 0.56$	
	3) 0.73	$0.437 \pm 0.072$	
Vipers	0.8	$0.47 \pm 0.08$	De la Torre et al (2013) [41]
2dFGRS	0.13	$0.46 \pm 0.06$	Percival et al. (2004) [42]
LRG	0.35	$0.445 \pm 0.097$	Chuang and Wang (2013) [43]
LOWZ	0.32	$0.384 \pm 0.095$	Chuang et al (2013) [44]
CMASS	0.57*	$0.348 \pm 0.071$	Beutler et al (2014) [35] Samushia et al (2014) [18] Reid et al (2013) [45]
	0.57*	$0.423 \pm 0.052$	
	0.57	$0.441 \pm 0.043$	
	0.57*	$0.450 \pm 0.011$	

TABLE I. Current published values of  $f\sigma_8(z)$ . In some cases we list also the correlation coefficient  $\rho_{ij}$  between different bins [17]. Entries with an asterisk are not employed in this analysis.

#### IV. CURRENT GROWTH-RATE DATA

Current growth data are not sufficient to provide  $k$ -dependent information. In this case, therefore, we are forced to neglect the  $k$ -dependence of  $Y$ . Moreover, again in view of the lack of sufficient statistics, we also fix the time dependence and assume that  $Y$  is just a constant over the redshift range of the observations. We have therefore just two parameters:  $\hat{Y}$  and the initial condition  $\alpha$ . We will consider four cases, in increasing order of “model independence”. The *first case* is standard  $\Lambda$ CDM gravity ( $Y = 1$ ), and  $\sigma_8$  and initial conditions both fixed to the fiducial model,  $\sigma_8 = 0.83$  [24] and  $\alpha = 1$ . Here the only free parameter is therefore  $\Omega_{m,0}$  (with an uniform prior in  $(0, 1)$ ). The *second case* is like the first one but with marginalization over  $\sigma_8$ . This case serves mainly to isolate the effect of the  $\sigma_8$ -marginalization and to see how much the best fit of  $\Omega_{m,0}$  changes if  $\sigma_8$  is estimated from the  $f\sigma_8(z)$  data themselves and not from Planck. From now on, we always fix the background evolution  $E$  to a  $\Lambda$ CDM with  $\Omega_{m,0}^{(bg)} = 0.3$ , in agreement with observations and close to the Planck best fit [24], and neglecting any uncertainty on it and we always include the marginalization over  $\sigma_8$ . In the *third case*, beside marginalizing over  $\sigma_8$ , we leave  $\hat{Y}$  free to vary with an uniform prior for positive values. Finally, the *fourth case* is like the third one but now the initial growth rate  $\alpha$  is left free to vary.

The results for the first and second cases are shown on the left panel of Fig. (1). At 68% c.l., the uncertainty on  $\Omega_{m,0}$  increases from 0.03 to roughly 0.10 when marginalizing over  $\sigma_8$  while for  $\sigma_8$  itself we find  $\sigma_8 = 0.76^{+0.06}_{-0.10}$ , smaller than but compatible with the Planck value. On the right panel, we plot the  $f\sigma_8$  data points from the galaxy surveys with their respective error bars in comparison with the  $\Lambda$ CDM model and with the best fits of all the cases.

In the third case (uniform prior on  $\hat{Y}$ , fixing  $\alpha = 1$ ) we find a best fit  $\hat{Y} = 0.20$  with an error range  $[0.095, 0.36]$  at 68% confidence level, see Fig. (2) bottom left panel. The parameter  $\sigma_8$  is now  $\sigma_8 = 0.79^{+0.11}_{-0.25}$ , see Fig. (3). If now we vary  $\alpha$  with a uniform prior on  $\hat{Y}$  (fourth case, Fig. 2) we obtain instead  $\hat{Y} = 0.28$  with a doubled error range  $[0.048, 0.63]$  at 68% c.l. . For  $\sigma_8$  we have now  $\sigma_8 = 0.54^{+0.21}_{-0.09}$ . Table (II) summarizes the results.

Interestingly, we detect a bimodality in the marginalized posterior for  $\alpha$  and a strong correlation with  $\hat{Y}$ . As shown in Fig. (2) both very large and very small values of  $\hat{Y}$  are acceptable if  $\alpha$  varies freely. In particular, a large  $\hat{Y}$  can be compensated by a large negative  $\alpha$ , while small  $\hat{Y}$  are compatible with large positive values. Large negative values of  $\alpha$  mean that overdensities can become underdensities at some point in time; although this might appear pathological at first sight, it does not contradict any observation at linear scales and should not be arbitrarily excluded. Within  $3\sigma$ , a small  $\hat{Y}$  is compatible with any value of  $\alpha$  since in this limit the perturbation equation becomes effectively first order in  $\delta'$ .

The conclusion of this section is that current data put hardly any constraint on  $\hat{Y}$ . Any value from 0 to 1.35 is acceptable at 95% and much larger values of  $\hat{Y}$  are also acceptable if the initial condition is chosen along the degeneracy line of Fig. (2).

This conclusion could have been reasonably expected due to the paucity of present data. In the next section we

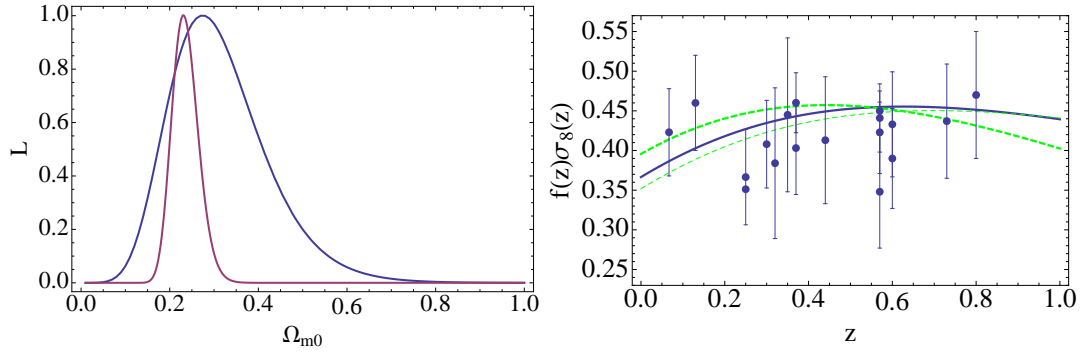


FIG. 1. *Left panel*: Current posterior in function of  $\Omega_{m,0}$  for  $\Lambda$ CDM model (first case). *Right panel*: Best fit  $\Lambda$ CDM model for the first case (blue solid curve); best fit for the third case (green thin dashed curve) and for the fourth case (green thick dashed curve) together with the entire set of  $f\sigma_8$  data points we employed in this paper. As the posterior is marginalized over  $\sigma_8$ , a possible vertical rescaling for the third and fourth cases is inconsequential so they have been plotted with a normalization that minimizes the  $\chi^2$  distance.

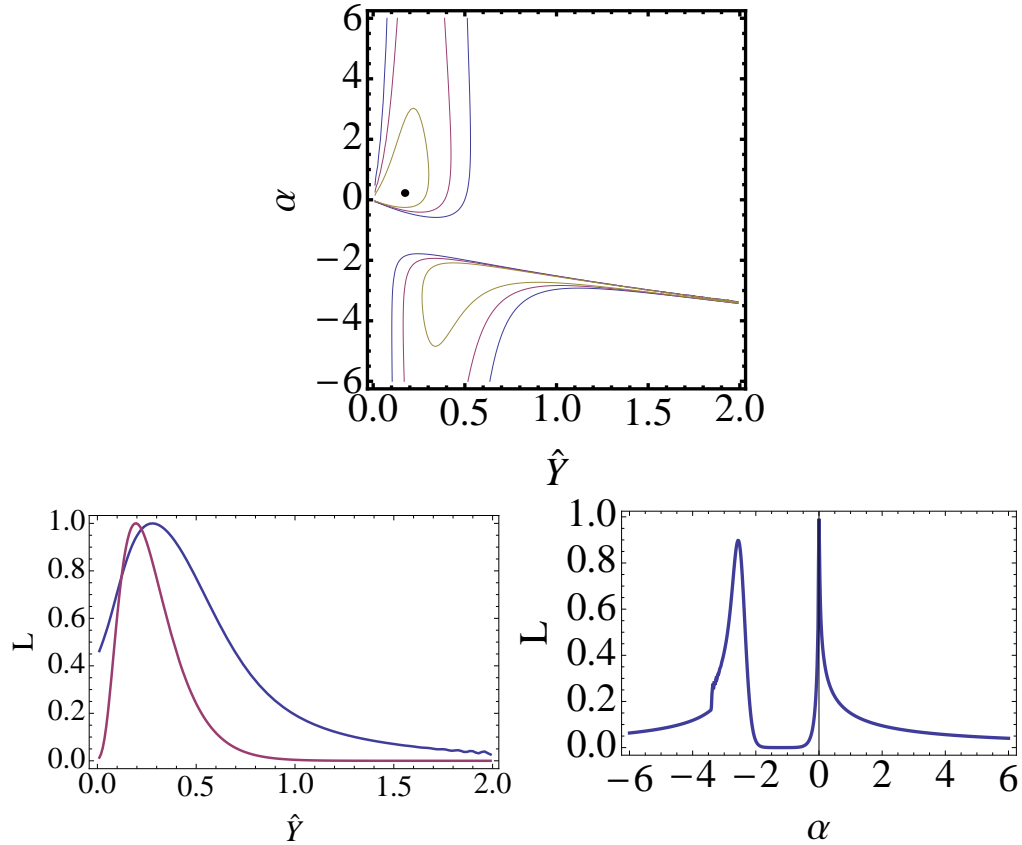


FIG. 2. *Top panel*:  $1\sigma$ ,  $2\sigma$  and  $3\sigma$  confidence-level contours for the 2-dimensional current posterior on the parameters  $\{\hat{Y}, \alpha\}$  marginalizing over  $\sigma_8$  (fourth case). *Left bottom panel*: Current posterior for  $\hat{Y}$  marginalized over  $\alpha$  (blue line) in comparison with the third case (red line). *Right bottom panel*: Current posterior for  $\alpha$  marginalized over  $\hat{Y}$ .

show however that the constraints improve a lot with the much better data of future surveys only if we keep  $\alpha$  fixed; in the more general case, the improvement remains modest. The reason is the same: trying to be as much model-independent as possible one has to set  $\sigma_8, \Omega_{m,0}, \alpha$  free to vary. The price to pay for this freedom are rather weak constraints.



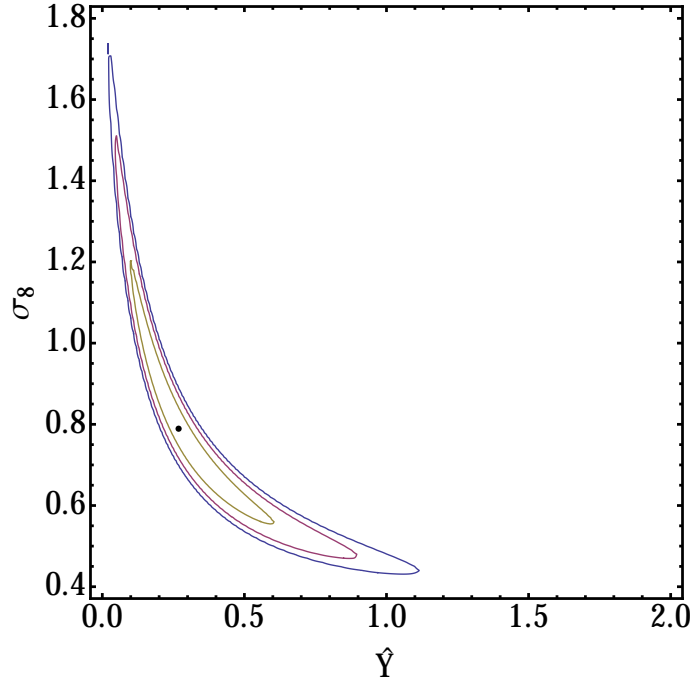


FIG. 3.  $1\sigma$ ,  $2\sigma$  and  $3\sigma$  confidence-level contours for the current posterior on the parameters  $\{\hat{Y}, \sigma_8\}$  (third case).

	case	$\alpha$ (best fit)	$\Delta\alpha$ (95%)	$\Delta\alpha$ (68%)	$\Omega_{m,0}^{(bg)}$ (best fit)	$\Delta\Omega_{m,0}^{(bg)}$ (95%)	$\Delta\Omega_{m,0}^{(bg)}$ (68%)
$\Lambda$ CDM, $Y = 1$ , $\sigma_8 = 0.83$	I	1	-	-	0.23	[0.18, 0.29]	[0.20, 0.26]
$\Lambda$ CDM, $Y = 1$ , marg. on $\sigma_8$	II	1	-	-	0.27	[0.12, 0.54]	[0.18, 0.39]
	case				$\hat{Y}$	$\Delta\hat{Y}$ (95%)	$\Delta\hat{Y}$ (68%)
Uniform prior on $\hat{Y}$	III	1	-	-	0.20	[0.040, 0.60]	[0.095, 0.36]
Uniform prior on $\hat{Y}, \alpha$	IV	-0.015	$\leq -2.08$ and $\geq -0.67$	$[-0.40, 1.32]$ and $[-4.05, -2.20]$	0.28	[0, 1.35]	[0.048, 0.63]

TABLE II. Summary of results for current data.

## V. FORECAST DATA

### A. $z$ BINNING

In this section we consider the forecast Euclid-like  $f\sigma_8$  datasets, starting with the case of no scale information ( $z$ -binning), which can be directly compared to the previous ones. The growth forecasts are obtained from Ref. [10]. We consider a Euclid-like 15,000 square degrees redshift survey from  $z = 0.5 - 1.5$  divided in equally spaced bins of width  $\Delta z = 0.2$  and, in order to prevent accidental degeneracy due to low statistic, a single larger redshift bin between  $z = 1.5 - 2.1$ , so in total we have six bins. In Table III we show the fiducial values and relative errors on  $f\sigma_8$ .

As before, we want to obtain an estimate on a constant  $\hat{Y}$  marginalizing over  $\sigma_8$  and  $\alpha$ . Fig. (4), lower left panel, shows the 1-dimensional marginalized *forecast posterior* distribution of  $Y$  (third case) along with the fourth case, i.e. with marginalization over  $\alpha$ . As can be seen from Fig. (4), lower left panel, the 95% error on  $\hat{Y}$  around the fiducial value 0.3 has a fivefold increase, from 0.03 to roughly 0.15, when we marginalize over the initial conditions. The relative uncertainty on  $\hat{Y}$  is around 30% at 68% c.l.. Contrary to what we found previously using current data, negative values of  $\alpha$  appear now strongly disfavoured.

The increase in errors on both  $\hat{Y}$  and  $\sigma_8$  can be appreciated from Fig. (5). In the third case (i.e. no marginalization over  $\alpha$ ) future Euclid-like data can estimate  $\sigma_8$  and  $\hat{Y}$  to within 0.01 for both parameters; when  $\alpha$  is marginalized

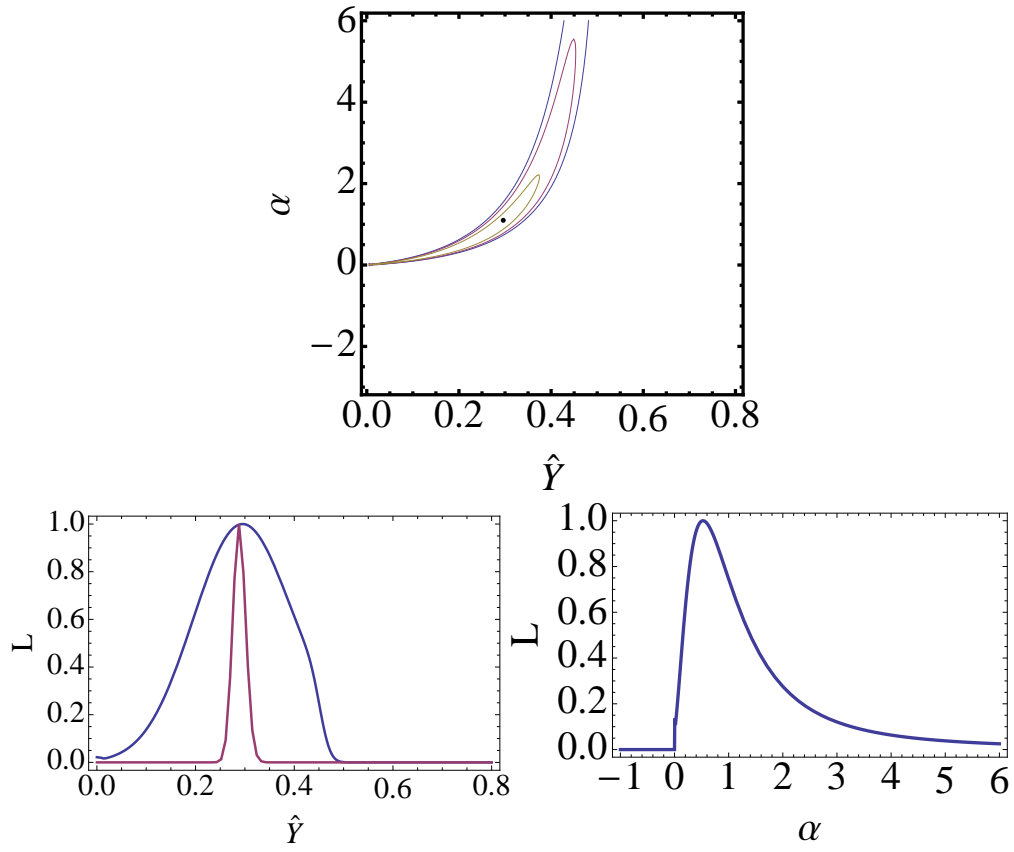


FIG. 4. *Top panel* :  $1\sigma$ ,  $2\sigma$  and  $3\sigma$  confidence-level contours for the 2-dimensional forecast posterior on the parameters  $\{\hat{Y}, \alpha\}$  marginalizing over  $\sigma_8$  (fourth case). *Left bottom panel* : forecast posterior for  $\hat{Y}$  marginalized over  $\alpha$  (blue line) in comparison with the third case (red line). *Right bottom panel* : forecast posterior for  $\alpha$  marginalized over  $\hat{Y}$

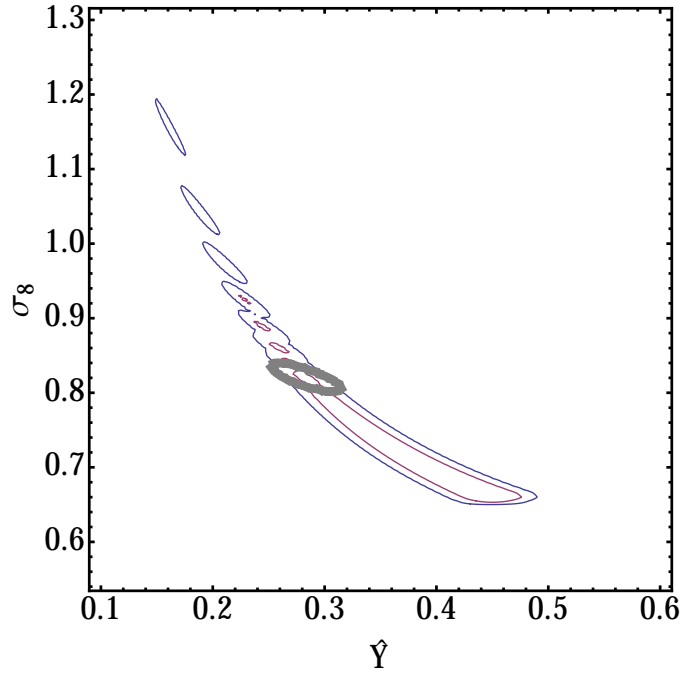


FIG. 5.  $1\sigma$  and  $2\sigma$  confidence-level contours for the forecast posterior on the parameters  $\{\hat{Y}, \sigma_8\}$  when  $\alpha$  is marginalized over (fourth case, solid curves) and when is fixed (third case, small gray ellipse, only the  $2\sigma$  contour is shown).



$\bar{z}$	$f\sigma_8$	$\Delta f\sigma_8$ (68% c.l.)
0.6	0.469	0.0092
0.8	0.457	0.0068
1.0	0.438	0.0056
1.2	0.417	0.0049
1.4	0.396	0.0047
1.8	0.354	0.0039

TABLE III. Fiducial values and Euclid-like errors for  $f\sigma_8$  using six redshift bins (from [10]).

	case	Best fit $\alpha$	$\Delta\alpha$ (95%)	$\Delta\alpha$ (68%)	Best fit $\hat{Y}$	$\Delta Y$ (95%)	$\Delta Y$ (68%)
Uniform prior on $\hat{Y}$	III	1	-	-	0.29	[0.26, 0.32]	[0.28, 0.30]
Uniform prior on $\hat{Y}, \alpha$	IV	0.53	[0, 4.0]	[0.12, 1.6]	0.30	[0.12, 0.43]	[0.21, 0.38]

TABLE IV. Summary of results for forecasted Euclid data.

over however the error increases to roughly 0.08, again for both parameters.

## B. $k$ BINNING

We consider now the quasi-static Horndeski result, defined in Eq. (4), which contains the parameters  $h_1, h_3$  and  $h_5$  and a  $k$ -dependence. Although in general these parameters depend on time, we assume here for simplicity that they time variation is negligible in the observed range. The aim of this section is to obtain error estimates on the Horndeski parameters, so we need to have a minimum of three  $k$ -bins for every value of the redshift. Again following the method of [10] we take the minimum binning value of  $k$  as  $k_{min} = 0.007 h/Mpc$  (the result is very weakly dependent on this value) and the values of the highest  $k$  are chosen to be well below the scale of non-linearity at the redshift of the bin. In Table V we report the  $k$ -bin boundaries.

In Table VI we display the fiducial values and errors for  $f\sigma_8$  at every redshift and every  $k$ -bin. As in the previous case, also here the fiducial model is chosen to be  $\Lambda$ CDM, so the fiducial values for the Horndeski parameters are  $\hat{h}_1 = \Omega_{m,0}h_1 = 0.3$  and  $h_3 = h_5 = 0$ . Here we fix  $h_5$  to its fiducial value (i.e. to zero) due to the degeneracy between  $h_5$  and  $h_3$  when the fiducial model is such that  $h_5 = h_3$  as in  $\Lambda$ CDM. In the next section we will consider the case in which the fiducial value of  $h_5$  is different from the standard value.

The model now contains three parameters:  $\{\hat{h}_1, h_3, \alpha\}$ . Note that in principle one should take a different  $\alpha$  for every  $k$  but for simplicity we assume that  $\alpha$  is  $k$ -independent in our range. As in the previous cases, here we analyze first the case in which  $\alpha = 1$  (this is our *fifth case*) and the case in which we will vary this parameter (*sixth case*). We numerically solve Eq. (1) inserting now the value of  $k$  corresponding to the central  $k$ -bin values for every redshift bin and then we construct the  $\sigma_8$ -marginalized three dimensional forecasted posterior by following the same procedure described in section III. The results are reported in Table VII and in Figs. (6,7). The error on  $\hat{h}_1$  increase from roughly 0.02 to 0.10 when marginalizing over the initial condition. In contrast, the error on the scale  $h_3$  remain practically unchanged, since we assume  $k$ -independent initial conditions.

$\bar{z}$	$k_{min} - k_1$	$k_1 - k_2$	$k_2 - k_{max}$
0.6	0.007-0.022	0.022-0.063	0.063-0.180
0.8	0.007-0.023	0.023-0.071	0.071-0.215
1.0	0.007-0.024	0.024-0.078	0.078-0.249
1.2	0.007-0.026	0.026-0.086	0.086-0.287
1.4	0.007-0.027	0.027-0.094	0.094-0.329
1.8	0.007-0.029	0.029-0.112	0.112-0.426

TABLE V. Ranges of the  $k$ -bins for every redshift bin centered at  $\bar{z}$ , in units of ( $h/Mpc$ ) (from [10]).

$\bar{z}$	$i$	$f\sigma_8(z)$	$\Delta f\sigma_8(z)$	$\Delta f\sigma_8(z)\%$
0.6	1	0.469	0.07	15
	2		0.017	3.6
	3		0.0097	2.1
0.8	1	0.457	0.05	11
	2		0.012	2.6
	3		0.0074	1.6
1.0	1	0.438	0.039	8.9
	2		0.0089	2
	3		0.0062	1.4
1.2	1	0.417	0.032	7.7
	2		0.0072	1.7
	3		0.0055	1.3
1.4	1	0.396	0.028	7
	2		0.0065	1.6
	3		0.0057	1.4
1.8	1	0.354	0.015	4.3
	2		0.0047	1.3
	3		0.0061	1.7

TABLE VI. Fiducial values and relative errors for  $f\sigma_8$  data at every redshift  $\bar{z}$  and every  $k$ -bin (labeled with the index  $i$ ).

	case	$\alpha$ (best fit)	$\Delta\alpha$ (95%)	$\Delta\alpha$ (68%)	$\hat{h}_1$ (best fit)	$\Delta\hat{h}_1$ (95%)	$\Delta\hat{h}_1$ (68%)	$h_3$ (best fit)	$\Delta h_3$ (95%)	$\Delta h_3$ (68%)
Horndeski	V	1	-	-	0.3	[0.26, 0.32]	[0.27, 0.32]	0	[-0.70, 0.72]	[-0.37, 0.35]
Horndeski	VI	0.85	[0.10, 2.2]	[0.22, 1.9]	0.3	[0.097, 0.44]	[0.17, 0.40]	0	[-0.72, 0.73]	[-0.36, 0.36]

TABLE VII. Best fit and errors on  $\hat{h}_1$ ,  $h_3$  in the Horndeski case by fixing  $h_5 = 0$ .

## VI. A COSMOLOGICAL EXCLUSION PLOT

Here we wish to continue the analysis by obtaining an exclusion plot, i.e. the region of parameter space that a future Euclid-like redshift survey can achieve. This is obtained by repeating the procedure of the previous section obtaining the errors on  $\hat{h}_1, h_3$  for every possible  $h_5$  (rather than fixing  $h_5$  to the standard value). The region outside the errors is therefore the region that an Euclid-like experiment will be able to rule out.

The form of  $Y$  in Eq. (4) produced in a Horndeski model represents a Yukawa-like gravitational potential in real space. By Fourier anti-transforming Eq. (2) with a point source of mass  $M$  one obtains in fact

$$\Psi(r) = -\frac{G_0 M}{r} h_1 \left(1 + Q e^{-r/\lambda}\right) \quad (13)$$

where  $h_5 = (1 + Q)\lambda^2$  and  $h_3 = \lambda^2$  (notice that here again  $Mh_1$  is the observable, not  $h_1$  alone). Here  $G_0$  is the gravitational constant one would measure in laboratory where, as already mentioned, the effects of the modification of gravity are assumed to be screened [46].

Thus, instead of  $h_{3,5}$ , we can use the strength  $Q$  and range  $\lambda$  of the Yukawa term as modified-gravity parameters, marginalizing over  $\hat{h}_1 = \Omega_{m,0} h_1$  and, as before, also over  $\sigma_8$  and  $\alpha$ . As previously, we assume  $Q, \lambda$  to be constant in the observed range. These parameters are the cosmological analog of the parameters employed in laboratory experiments to test deviations from Newtonian gravity, see e.g. [47]. Using the same specifications of the previous section, we show in Fig. (8) the region that a Euclid-like experiment is able to exclude. Clearly, for very small  $\lambda$  the strength  $Q$  is unconstrained; moreover, for very large interaction ranges (much larger than the observed scales), the strength becomes degenerate with  $h_1$  and therefore again weakly constrained. In the intermediate region around 10 Mpc/ $h$  the strength can be confined to within 0.03 (0.06) at 68% (95%) c.l., i.e. 3% (6%) of the Newtonian gravitational strength. This limit is of course much weaker than local gravity bounds, which are below  $10^{-4}$ , but it applies to scales and epochs unreachable with other means. The results will not change much if we do not marginalize over initial conditions, just as it happened for  $h_3$  in the previous section.

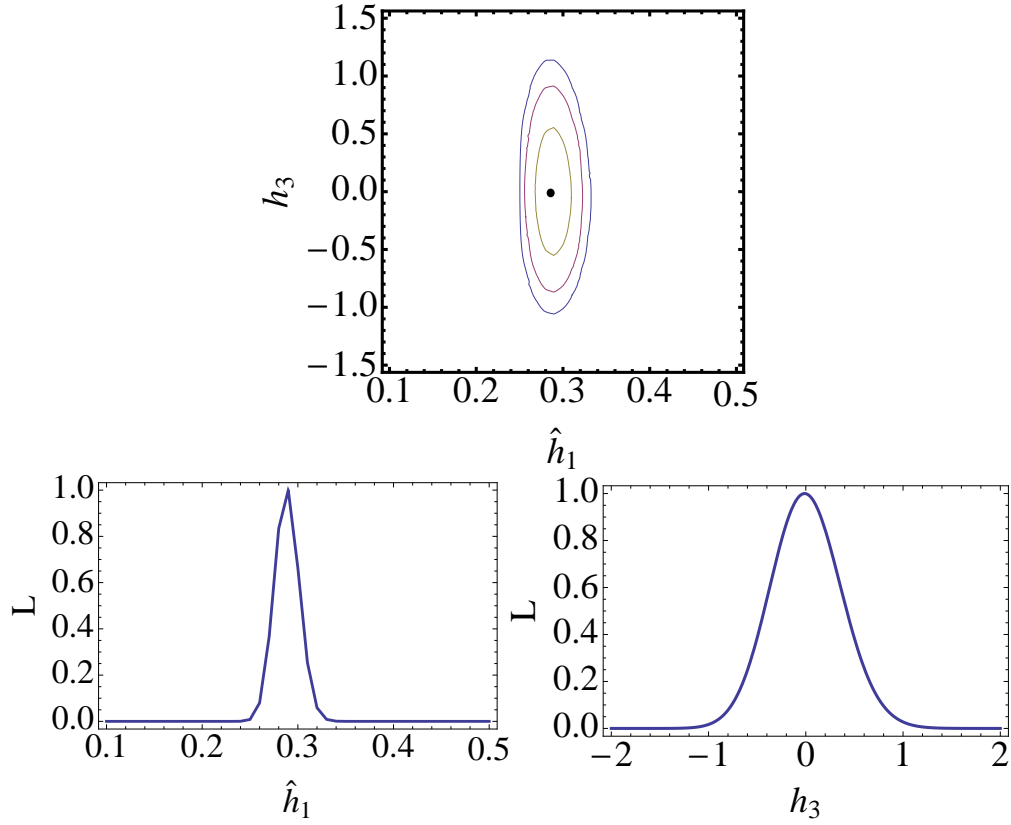


FIG. 6. *Top panel* :  $1\sigma$ ,  $2\sigma$  and  $3\sigma$  confidence-level contours for the 2-dimensional forecast posterior on the parameters  $\{\hat{h}_1, h_3\}$  marginalizing over  $\sigma_8$  (fifth case). *Left bottom panel* : forecast posterior for  $\hat{h}_1$  marginalized over  $h_3$ . *Right bottom panel* : forecast posterior for  $h_3$  marginalized over  $\hat{h}_1$ .

For comparison, the strength  $Q$  in the case of  $f(R)$  models is  $1/3$  (see e.g. [48]), while the range is

$$\lambda_{f(R)} = M_{f(R)}^{-1} = \sqrt{\frac{3f_{,RR}}{f_{,R}}} \quad (14)$$

where the subscripts denote the derivative with respect to  $R$  of the Lagrangian  $f(R)$  (in this notation  $f(R)$  includes the Einstein-Hilbert term). From Fig. (8) one can see that all the models with  $2 \lesssim \lambda_{f(R)} \lesssim 80 \text{ Mpc}/h$  could be ruled out at 95% c.l. for  $Q = 1/3$ . Conversely, assuming  $f_{,R} \approx 1$  as needed by local gravity constraints and by a background close to  $\Lambda\text{CDM}$ , a Euclid-like survey will be able to set a lower and an upper limit to  $f_{,RR}$ :

$$f_{,RR} < 1 \cdot 10^{-7} H_0^{-2}, \quad \text{or} \quad (15)$$

$$f_{,RR} > 2 \cdot 10^{-4} H_0^{-2} \quad (16)$$

In keeping with our analysis, we are assuming here  $\lambda_{f(R)}$  constant; in general however it will be a function of time so these limits should refer to the epoch of observation. In some popular models of  $f(R)$  one has  $f_{,RR} \approx 10^{-3} H_0^{-2}$  at  $z \approx 1$  (see e.g. [49]), corresponding to  $\lambda_{f(R)} \approx 100 - 200 \text{ Mpc}/h$ , a value that could be marginally detected at 68% c.l. by our forecasts.

Notice however that in  $f(R)$  models the overall factor here denoted as  $\hat{h}_1$  corresponds to  $\Omega_{m,0}/f_{,R} \approx \Omega_{m,0}$ . The existence of a lower limit to  $f_{,RR}$  is due to the marginalization over the unknown  $\Omega_{m,0}$ . In specific models of  $f(R)$  the present matter density  $\Omega_{m,0}$  can be estimated through background or large-scale structure measurements. In this case the lower limit would be removed and any  $\lambda_{f(R)}$  larger than a few Megaparsec would be detected. The application of the results of this paper to specific models of modified gravity is left to future work.

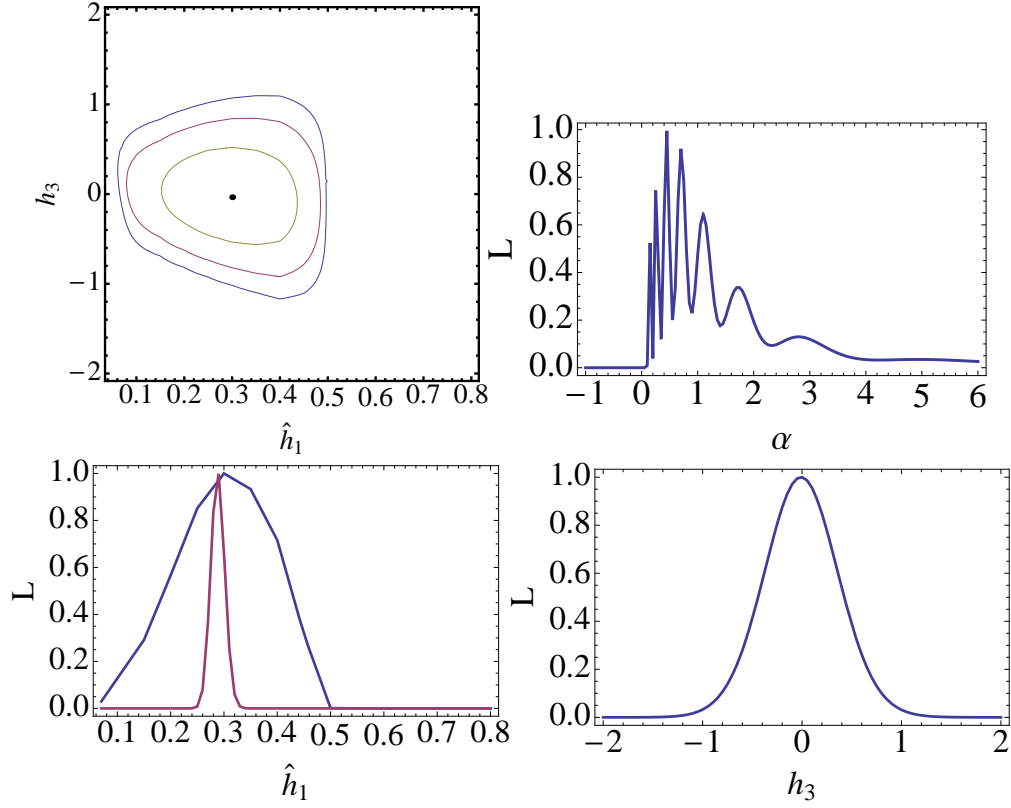


FIG. 7. *Top panel* :  $1\sigma$ ,  $2\sigma$  and  $3\sigma$  confidence-level contours for the 2-dimensional forecast posterior on the parameters  $\{\hat{h}_1, h_3\}$  marginalizing on  $\{\sigma_8, \alpha\}$  (sixth case). *Left bottom panel* : forecast posterior marginalized on  $\{h_3, \alpha\}$  varying the initial conditions (blue line) in comparison with the fifth case (red line). *Right bottom panel* : forecast posterior marginalized on  $\{\hat{h}_1, \alpha\}$

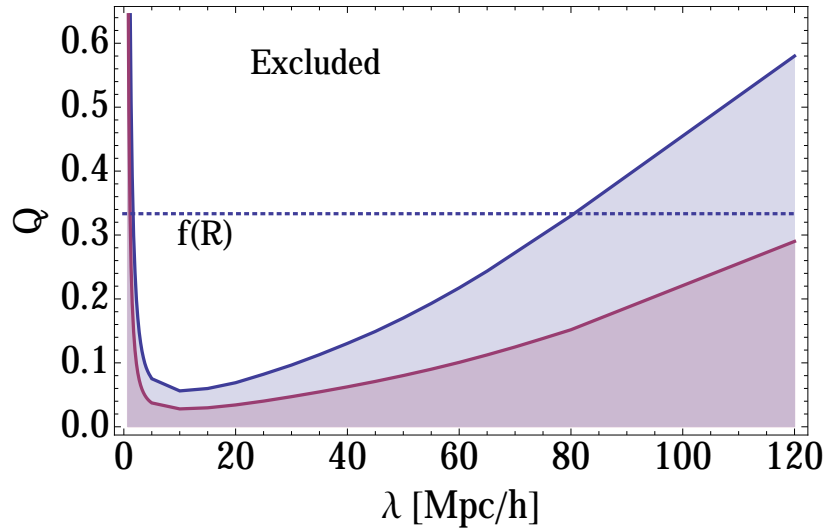


FIG. 8. Forecast of a cosmological exclusion plot for a Euclid-like survey, marginalizing over  $\sigma_8, \alpha$  and  $\hat{h}_1$ . Here  $Q$  is the dimensionless strength of the Yukawa interaction while  $\lambda$ , in  $\text{Mpc}/h$ , is the interaction range. The darker region is the 68% c.l. region, the lighter one is the 95% c.l. region. The dotted line marks the value of  $Q$  in  $f(R)$  models.

## VII. CONCLUSIONS

In this paper we investigated the current and future bounds on the modified gravity parameter  $Y$  (or  $G_{\text{eff}}$ ) that quantifies the deviation from the standard Poisson equation. We have assumed  $Y$  to be constant in time and space when using current data or with a Horndeski behavior when forecasting future results. Contrary to other similar analyses, we tried to weaken the model-dependency by marginalizing over the present power spectrum normalization  $\sigma_8$  and over the initial growth rate for the matter density contrast equation, since they both are unknown unless one assumes a specific model, e.g.  $\Lambda$ CDM. We also take into account the fact that  $\Omega_{m,0}$  is not a directly observable quantity and absorb it into the definition of  $Y$ .

We find, not unexpectedly, that the current growth rate data  $f\sigma_8(z)$  from redshift distortion are insufficient to constrain the product  $\hat{Y} = \Omega_{m,0}Y$  to better than an order of 100% error (see Table II, fourth case), due to the degeneracy with  $\sigma_8$  and the initial condition. Using instead forecasts of a Euclid-like experiment, we find that the relative error on  $\Omega_{m,0}Y$  reduce to roughly 30% at 68% c.l. (see Table IV, fourth case). A similar error can be obtained on  $\hat{h}_1 = \Omega_{m,0}h_1$  when using the Horndeski prescription (see Table VII, sixth case). The effect of the lack of knowledge of the initial conditions can be easily grasped by noting that the uncertainty on  $\hat{Y}$  increases from  $\Delta\hat{Y} \approx 0.01$  when  $\alpha = 1$  to  $\Delta\hat{Y} \approx 0.08$  when  $\alpha$  is marginalized over (Table II), i.e. from a few percent to 30%. Same broadening of the uncertainty occurs for  $\sigma_8$ .

Finally, we obtain a forecast of a cosmological exclusion plot on the Yukawa strength  $Q$  and range  $\lambda$  parameters (Fig. 8). This complements, on cosmological scales, the laboratory exclusion plots on deviations from standard gravity. We find that with a Euclid-like experiment the strength  $Q$  can be confined to within 3%(6%) of the Newtonian gravity at 68%(95%) if the interaction range is around 10 Megaparsecs. For much larger and much smaller ranges the constraint gradually vanishes. Applying these results to  $f(R)$  models we forecast an upper limit to  $f_{,RR}$  at  $z \approx 1$  of the order of  $10^{-7}H_0^{-2}$ , corresponding to a Yukawa range smaller than 2 Mpc/ $h$  roughly, and a lower limit of  $2 \cdot 10^{-4}H_0^{-2}$ , corresponding to scales larger than 80Mpc/ $h$  (at 95% c.l.).

The main conclusion of this paper is that  $Y$  can be only weakly constrained by the next decade redshift surveys if one takes into account the degeneracy with  $\sigma_8$ ,  $\Omega_{m,0}$  and initial conditions. Even weaker constraints would have been obtained had we taken  $Y$  to be time dependent. Only by considering specific models can one hope to produce stringent constraints on modified gravity through its effect on linear matter perturbation growth. This seems to indicate that the other modified gravity linear perturbation parameter, the anisotropic stress  $\eta$ , which requires a combination of weak lensing and clustering, is a more robust and powerful way to quantify the deviation from standard gravity.

## ACKNOWLEDGMENTS

L.A. acknowledges support from DFG through the project TRR33 “The Dark Universe”. We thank Alejandro Guarnizo-Trilleras and Adrian Vollmer for help with the forecasts and Guillermo Ballesteros, Emilio Bellini, Valerio Marra and Valeria Pettorino for useful discussions. L.T. thanks the Institute of Theoretical Physics at the University of Heidelberg for the hospitality.

- 
- [1] Gregory Walter Horndeski, “Second-order scalar-tensor field equations in a four-dimensional space,” *Int.J.Th.Phys.* **10**, 363–384 (1974).
  - [2] L. Amendola, M. Kunz, and D. Sapone, “Measuring the dark side (with weak lensing),” *JCAP* **4**, 013 (2008), [arXiv:0704.2421](#).
  - [3] Antonio De Felice, Tsutomu Kobayashi, and Shinji Tsujikawa, “Effective gravitational couplings for cosmological perturbations in the most general scalar-tensor theories with second-order field equations,” *Phys.Lett.* **B706**, 123–133 (2011), [arXiv:1108.4242 \[gr-qc\]](#).
  - [4] Alessandra Silvestri, Levon Pogosian, and Roman V. Buniy, “A practical approach to cosmological perturbations in modified gravity,” (2013), [arXiv:1302.1193 \[astro-ph.CO\]](#).
  - [5] J. Zuntz, T. Baker, P. G. Ferreira, and C. Skordis, “Ambiguous tests of general relativity on cosmological scales,” *J. Cosmology Astropart. Phys.* **6**, 032 (2012), [arXiv:1110.3830 \[astro-ph.CO\]](#).
  - [6] Frank Könnig, Yashar Akrami, Luca Amendola, Mariele Motta, and Adam R. Solomon, “Stable and unstable cosmological models in bimetric massive gravity,” (2014), [arXiv:1407.4331 \[astro-ph.CO\]](#).
  - [7] S.F. Hassan and Rachel A. Rosen, “Resolving the Ghost Problem in non-Linear Massive Gravity,” *Phys.Rev.Lett.* **108**, 041101 (2012), [arXiv:1106.3344 \[hep-th\]](#).
  - [8] Antonio De Felice and Shinji Tsujikawa, “Conditions for the cosmological viability of the most general scalar-tensor theories and their applications to extended Galileon dark energy models,” *JCAP* **1202**, 007 (2012), [arXiv:1110.3878 \[gr-qc\]](#).

- [9] L. Amendola, M. Kunz, M. Motta, I. D. Saltas, and I. Sawicki, “Observables and unobservables in dark energy cosmologies,” *Phys. Rev. D* **87**, 023501 (2013), [arXiv:1210.0439 \[astro-ph.CO\]](#).
- [10] Luca Amendola, Simone Fogli, Alejandro Guarnizo, Martin Kunz, and Adrian Vollmer, “Model-independent constraints on the cosmological anisotropic stress,” *Phys.Rev.* **D89**, 063538 (2014), [arXiv:1311.4765 \[astro-ph.CO\]](#).
- [11] Michael Doran and Georg Robbers, “Early dark energy cosmologies,” *JCAP* **0606**, 026 (2006), [arXiv:astro-ph/0601544](#).
- [12] V. Pettorino, L. Amendola, and C. Wetterich, “How early is early dark energy?” [arXiv:1301.5279 \(2013\)](#), [arXiv:1301.5279 \[astro-ph.CO\]](#).
- [13] Y. Gong, “Growth factor parametrization and modified gravity,” *Phys. Rev. D* **78**, 123010 (2008), [arXiv:0808.1316](#).
- [14] Tatsuya Narikawa and Kazuhiro Yamamoto, “Characterizing the linear growth rate of cosmological density perturbations in an  $f(R)$  model,” *Phys. Rev.* **D81**, 043528 (2010), [arXiv:0912.1445 \[astro-ph.CO\]](#).
- [15] Koichi Hirano, Zen Komiya, and Hisato Shirai, “Constraining Galileon gravity from observational data with growth rate,” *Prog.Theor.Phys.* **127**, 1041–1056 (2012), [arXiv:1103.6133 \[astro-ph.CO\]](#).
- [16] K. Shi, Y.F. Huang, and T. Lu, “Constraining dark energy using observational growth rate data,” *Phys.Lett.* **B717**, 299–306 (2012), [arXiv:1209.5580 \[astro-ph.CO\]](#).
- [17] Edward Macaulay, Ingunn Kathrine Wehus, and Hans Kristian Eriksen, “A Lower Growth Rate from Recent Redshift Space Distortions than Expected from Planck,” (2013), [arXiv:1303.6583 \[astro-ph.CO\]](#).
- [18] Lado Samushia, Beth A. Reid, Martin White, Will J. Percival, Antonio J. Cuesta, *et al.*, “The Clustering of Galaxies in the SDSS-III Baryon Oscillation Spectroscopic Survey (BOSS): measuring growth rate and geometry with anisotropic clustering,” (2013), [10.1093/mnras/stu197](#), [arXiv:1312.4899 \[astro-ph.CO\]](#).
- [19] Natalia A. Arkhipova, Olga Avsajanishvili, Tina Kahnishvili, and Lado Samushia, “Growth Rate in the Dynamical Dark Energy Models,” (2014), [arXiv:1406.0407 \[astro-ph.CO\]](#).
- [20] H. Steigerwald, J. Bel, and C. Marinoni, “Probing non-standard gravity with the growth index: a background independent analysis,” *J. Cosmology Astropart. Phys.* **5**, 042 (2014), [arXiv:1403.0898 \[astro-ph.CO\]](#).
- [21] Martin Kunz and Domenico Sapone, “Dark Energy versus Modified Gravity,” *Phys.Rev.Lett.* **98**, 121301 (2007), [arXiv:astro-ph/0612452 \[astro-ph\]](#).
- [22] Surhud More, Hironao Miyatake, Rachel Mandelbaum, Masahiro Takada, David Spergel, *et al.*, “The Weak Lensing Signal and the Clustering of BOSS Galaxies: Cosmological Constraints,” (2014), [arXiv:1407.1856 \[astro-ph.CO\]](#).
- [23] D. Rapetti, C. Blake, S. W. Allen, A. Mantz, D. Parkinson, and F. Beutler, “A combined measurement of cosmic growth and expansion from clusters of galaxies, the CMB and galaxy clustering,” *MNRAS* **432**, 973–985 (2013), [arXiv:1205.4679 \[astro-ph.CO\]](#).
- [24] P.A.R. Ade *et al.* (Planck Collaboration), “Planck 2013 results. XVI. Cosmological parameters,” [arXiv:1303.5076 \(2013\)](#), [arXiv:1303.5076 \[astro-ph.CO\]](#).
- [25] Planck Collaboration, P. A. R. Ade, N. Aghanim, C. Armitage-Caplan, M. Arnaud, M. Ashdown, F. Atrio-Barandela, J. Aumont, C. Baccigalupi, A. J. Banday, and *et al.*, “Planck 2013 results. XX. Cosmology from Sunyaev-Zeldovich cluster counts,” *ArXiv e-prints* (2013), [arXiv:1303.5080 \[astro-ph.CO\]](#).
- [26] L. Amendola and D. Tocchini-Valentini, “Stationary dark energy: The present universe as a global attractor,” *Phys. Rev. D* **64**, 043509 (2001), [arXiv:astro-ph/0011243](#).
- [27] H. Nariai, “Gravitational Instability in the Brans-Dicke Cosmology,” *Progress of Theoretical Physics* **42**, 544–554 (1969).
- [28] [Http://www.euclid-ec.org](http://www.euclid-ec.org).
- [29] R. Laureijs, J. Amiaux, S. Arduini, J. . Auguères, J. Brinchmann, R. Cole, M. Cropper, C. Dabin, L. Duvet, A. Ealet, and *et al.*, “Euclid Definition Study Report,” *ArXiv e-prints* (2011), [arXiv:1110.3193 \[astro-ph.CO\]](#).
- [30] Ippocratis D. Saltas, Ignacy Sawicki, Luca Amendola, and Martin Kunz, “Scalar anisotropic stress as signature of correction to gravitational waves,” (2014), [arXiv:1406.7139 \[astro-ph.CO\]](#).
- [31] Will J Percival and Martin White, “Testing cosmological structure formation using redshift-space distortions,” *Mon.Not.Roy.Astron.Soc.* **393**, 297–308 (2009), [arXiv:0808.0003 \[astro-ph\]](#).
- [32] Luca Amendola, Martin Kunz, Mariele Motta, Ippocratis D. Saltas, and Ignacy Sawicki, “Observables and unobservables in dark energy cosmologies,” *Phys.Rev.* **D87**, 023501 (2013), [arXiv:1210.0439 \[astro-ph.CO\]](#).
- [33] Luca Amendola, Guillermo Ballesteros, and Valeria Pettorino, “Effects of modified gravity on B-mode polarization,” (2014), [arXiv:1405.7004 \[astro-ph.CO\]](#).
- [34] Marco Raveri, Carlo Baccigalupi, Alessandra Silvestri, and Shuang-Yong Zhou, “Measuring the speed of cosmological gravitational waves,” (2014), [arXiv:1405.7974 \[astro-ph.CO\]](#).
- [35] Florian Beutler *et al.* (BOSS Collaboration), “The clustering of galaxies in the SDSS-III Baryon Oscillation Spectroscopic Survey: Testing gravity with redshift-space distortions using the power spectrum multipoles,” (2013), [arXiv:1312.4611 \[astro-ph.CO\]](#).
- [36] Luca Amendola *et al.* (Euclid Theory Working Group), “Cosmology and fundamental physics with the Euclid satellite,” *Living Rev.Rel.* **16**, 6 (2013), [arXiv:1206.1225 \[astro-ph.CO\]](#).
- [37] Florian Beutler, Chris Blake, Matthew Colless, D. Heath Jones, Lister Staveley-Smith, *et al.*, “The 6dF Galaxy Survey:  $z = 0$  measurement of the growth rate and  $\sigma_8$ ,” *Mon.Not.Roy.Astron.Soc.* **423**, 3430–3444 (2012), [arXiv:1204.4725 \[astro-ph.CO\]](#).
- [38] Lado Samushia, Will J. Percival, and Alvis Raccanelli, “Interpreting large-scale redshift-space distortion measurements,” *Mon.Not.Roy.Astron.Soc.* **420**, 2102–2119 (2012), [arXiv:1102.1014 \[astro-ph.CO\]](#).
- [39] Rita Tojeiro, W.J. Percival, J. Brinkmann, J.R. Brownstein, D. Eisenstein, *et al.*, “The clustering of galaxies in the SDSS-III Baryon Oscillation Spectroscopic Survey: measuring structure growth using passive galaxies,” *Mon.Not.Roy.Astron.Soc.* **424**, 2339–2344 (2012), [arXiv:1203.6565 \[astro-ph.CO\]](#).

- [40] Chris Blake, Sarah Brough, Matthew Colless, Carlos Contreras, Warrick Couch, *et al.*, “The WiggleZ Dark Energy Survey: Joint measurements of the expansion and growth history at  $z \lesssim 1$ ,” *Mon.Not.Roy.Astron.Soc.* **425**, 405–414 (2012), [arXiv:1204.3674 \[astro-ph.CO\]](#).
- [41] S. de la Torre, L. Guzzo, J.A. Peacock, E. Branchini, A. Iovino, *et al.*, “The VIMOS Public Extragalactic Redshift Survey (VIPERS). Galaxy clustering and redshift-space distortions at  $z=0.8$  in the first data release,” (2013), [arXiv:1303.2622 \[astro-ph.CO\]](#).
- [42] Will J. Percival *et al.* (2dFGRS Collaboration), “The 2dF Galaxy Redshift Survey: Spherical harmonics analysis of fluctuations in the final catalogue,” *Mon.Not.Roy.Astron.Soc.* **353**, 1201 (2004), [arXiv:astro-ph/0406513 \[astro-ph\]](#).
- [43] Chia-Hsun Chuang and Yun Wang, “Modeling the Anisotropic Two-Point Galaxy Correlation Function on Small Scales and Improved Measurements of  $H(z)$ ,  $D_A(z)$ , and  $\beta(z)$  from the Sloan Digital Sky Survey DR7 Luminous Red Galaxies,” *Mon.Not.Roy.Astron.Soc.* **435**, 255–262 (2013), [arXiv:1209.0210 \[astro-ph.CO\]](#).
- [44] Chia-Hsun Chuang, Francisco Prada, Florian Beutler, Daniel J. Eisenstein, Stephanie Escoffier, *et al.*, “The clustering of galaxies in the SDSS-III Baryon Oscillation Spectroscopic Survey: single-probe measurements from CMASS and LOWZ anisotropic galaxy clustering,” (2013), [arXiv:1312.4889 \[astro-ph.CO\]](#).
- [45] Beth A. Reid, Hee-Jong Seo, Alexie Leauthaud, Jeremy L. Tinker, and Martin White, “A 2.5% small-scale redshift space clustering of SDSS-III CMASS galaxies,” (2014), [arXiv:1404.3742 \[astro-ph.CO\]](#).
- [46] Notice that although one could define a new gravitational “constant”  $G_{\text{eff}} = G_0 h_1 (1 + Q e^{-r/\lambda})$  in the potential, one should use a different definition, namely  $G_{\text{eff}}^F = G_0 h_1 (1 + Q e^{-r/\lambda} (1 + r/\lambda))$ , in the force. This is why we prefer to use a different notation, i.e.  $Y$ .
- [47] D. J. Kapner, T. S. Cook, E. G. Adelberger, J. H. Gundlach, B. R. Heckel, C. D. Hoyle, and H. E. Swanson, “Tests of the Gravitational Inverse-Square Law below the Dark-Energy Length Scale,” *Physical Review Letters* **98**, 021101 (2007), [hep-ph/0611184](#).
- [48] Antonio De Felice and Shinji Tsujikawa, “f(R) theories,” *Living Rev.Rel.* **13**, 3 (2010), [arXiv:1002.4928 \[gr-qc\]](#).
- [49] L. G. Jaime, L. Patino, and M. Salgado, “f(R) Cosmology revisited,” *ArXiv e-prints* (2012), [arXiv:1206.1642 \[gr-qc\]](#).